Composites: Part B 45 (2013) 1620–1628

Contents lists available at SciVerse ScienceDirect

Composites: Part B

journal homepage: www.elsevier.com/locate/compositesb

Experimental and numerical investigation on bolted composite joint made by vacuum assisted resin injection

Song Zhou [a,*], Zhenqing Wang [a], Jiansheng Zhou [a], Xiaodi Wu [b]

[a] Smart Structures and Advanced Composites Laboratory, College of Aerospace and Civil Engineering, Harbin Engineering University, Harbin, China
[b] College of Power and Energy Engineering, Harbin Engineering University, Harbin, China

ARTICLE INFO

Article history:
Received 18 June 2012
Received in revised form 27 August 2012
Accepted 31 August 2012
Available online 27 September 2012

Keywords:
A. Laminates
B. Fracture
C. Finite element analysis (FEA)
E. Joints/joining

ABSTRACT

In this paper, experiments and finite element simulation were used to investigate the influence of geometric parameters on failure response of bolted single-lap composite joint. Specimens used for testing material stiffness, strength and failure of bolted single-lap composite joints were made by vacuum assisted resin injection (VARI). Two kinds of progressive failure models developed in ABAQUS/Standard and Explicit were used to simulate failure of joints. User subroutines USDFLD and VUMAT were used in these two models, respectively. Two finite element models showed an excellent agreement with experimental results. The results of the numerical analysis were presented with a focus on providing a more detailed insight into the progressive failure process, and the influence of the geometric parameter on failure of bolted composite single-lap joint. Failure model developed in ABAQUS/Explicit was found to be robust, accurate and highly efficient.

1. Introduction

Composite materials have a wide application in aerospace, ship building and civil engineering due to their high mechanical properties and low weights. In practical application, composite components are often fastened to other structural members by bolted joints [1,2]. Since composite bolted joints need to be drilled in laminate, large stress concentration tends to develop around the hole, which can severely reduce the overall strength of the structure. Bolted joints become very critical part of the structure, it is therefore important to design them safely [3]. Common failure modes in bolted composite joints are shown in Fig. 1.

To predict the failure of composite joints precisely, many researchers spent a lot of efforts in this field. There are many factors which can effect the failure of bolted composite joints, including stacking sequence, clamping force, bolt-hole clearance, friction and geometric parameters, etc. [4–18]. Wang [4] used Extended Finite Element Method (XFEM) to investigate failure of bolted single-lap composite joint. Crack of laminate could be observed clearly by XFEM. McCarthy et al. [5,6] used experiments and three-dimensional finite element models to study the effects of bolt–hole clearance on the single-bolt, single-lap composite (graphite/epoxy) joints. Simulation results were in close agreement with experiments, and experiments showed that increased clearance lead to increased bolt rotation, decreased bolt-hole contact area, and decreased joint stiffness. For multi-bolt composite joints, McCarthy et al. [7,8] used a global bolted joint model (GBJM) and an analytical model to investigate the bolt–hole clearance, bolt-torque, friction between laminates, secondary and tertiary bending in the laminates as well as the load distribution in multi-bolt joints, respectively. Since GBJM simplified the simulation, so the GBJM was found to be robust, accurate and highly efficient, with time savings of up to 97% realized over full three-dimensional finite element models. The analytical model was validated against detailed three-dimensional finite element models and experimental results. Sen et al. [9] analyzed failure of mechanically fastened joints with clearance in composite laminates under preload. The research focused on the failure experiments of composite mechanical fasten joint, the influences of clearance on failure load and failure mode. Kapti et al. [10] carried out experimental and numerical failure analysis of carbon/epoxy laminated composite joints under different conditions. Finite element models of the joints were also developed by using ANSYS software, and the simulations of bearing strength of joints could be verified by experiments. Other researchers paid more attention to failure criterion of composite to predict the progressive failure of joint. For instance, Santiuste and Olmedo [11] adopted Chang-Lessare criterion to study the progressive failure of joint. Lu et al. [12] presented a new method based on combination of the point estimate method (PEM) and Edgeworth series to estimate the probabilistic strength of the fastened joint in laminated composites. Dano et al. [13,14] used a finite element model with Hashin and the maximum stress failure criterion to predict progressive ply failure. Hühne et al. [15] employed a finite element

* Corresponding author. Tel./fax: +86 0451 82589364.
E-mail address: zhousongb09@hrbeu.edu.cn (S. Zhou).

1359-8368/$ - see front matter Crown Copyright © 2012 Published by Elsevier Ltd. All rights reserved.
http://dx.doi.org/10.1016/j.compositesb.2012.08.025

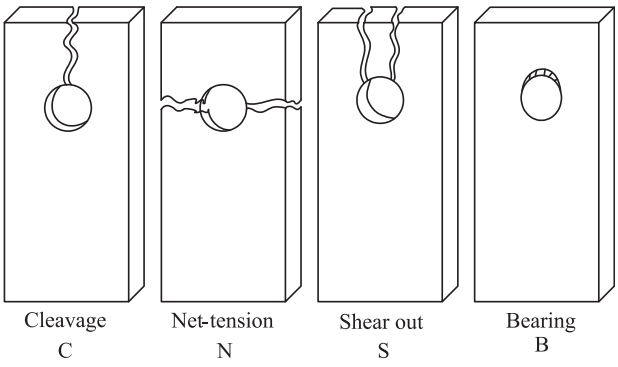

Fig. 1. Common failure modes in bolted composite plates.

model with Hashin's three-dimensional failure criterion and a constant degradation model to predict the failure of hybrid joint. All these finite element models had better agreements with experimental results. Feo et al. [16–18] investigated the failure of GFRP bolted laminates by numerical and experimental methods.

Although there are various research methods for failure of bolted composite joint, the laminates of joints are usually made by autoclave molding process which is limited by component size in application. With the wide application of composite, composite structures have more and more large size, and the disadvantage of autoclave molding process make it less use in the large composite structures. Meanwhile, a new process is introduced to make the GRP body. This is now formed by the vacuum assisted resin injection process (VARI). Since VARI process cures in room temperature and enable the manufacture of large structures with high mechanical properties under vacuum [19,20]. So vacuum assisted resin injection process (VARI) can be widely used in the large components, especially in the ship building. For example Visby class corvette was made by VARI process, as the first complete composite corvette, Visby had excellent stealth performance. For the anisotropy of composite and connection of large composite components, failure response analysis of composite joint made by VARI became quite important.

In this study, experiments and finite element simulation were used to investigate the influence of geometric parameters on failure response of bolted single-lap composite joint. Geometric parameters were the distance from the free edge of plate to the diameter of bolt hole (E/D) ratio and the width of the specimen to the diameter of bolt holes (W/D) ratios. In the experiments, specimens used for testing material stiffness, strength and failure of bolted single-lap composite joints were made by VARI process.

In numerical analysis, since the joint finite element problem was a contact problem which was a three-dimension finite element problem, however, traditional composite laminate was treated as shell element, which could not solve 3D element well. In this paper, 3D Hashin failure criteria was chosen for finite element analysis of composite joints. Two kinds of progressive failure models developed in ABAQUS/Standard and Explicit were used to simulate failure of joints. User subroutines USDFLD and VUMAT were used in these two models, respectively. In subroutine USDFLD, stiffness degradation occurred when failure criteria was satisfied. In subroutine VUMAT, once failure criteria was satisfied, stiffness degradation occurred, and the stress was calculated by subroutine. Two finite element models showed an excellent agreement with experimental results. Compared with finite element model developed in ABAQUS/Standard, model developed in ABAQUS/Explicit with subroutine VUMAT is introduced in this paper. Explicit model was found to could improve the convergence speed and reduce the computation time. The results of the numerical analysis were presented with a focus on providing a more detailed insight into the progressive failure process.

2. Experimental analysis

In this section, experiment program was conducted to obtain stiffness and strength properties of laminate and investigate the influence of geometric parameters on failure of bolted single-lap composite joint. Test specimens were made by glass/unsaturated polyester resin system using VARI process. VARI process was shown in Fig. 2. During the VARI process, the mold should be cleaned up, and then release agent was evenly coated on mold surface. Dry glass fiber was placed in the mold, then peel ply and flow media were placed on the fiber. The mold was closed by vacuum bag and sealant. After the preparation work was finished, Resin flowed into the mold and impregnated the glass fiber. The driving force for the flow of the resin was a pressure difference made by vacuum pump, when the pressure difference was big enough, vacuum pump would be shut down, and resin flowed into mold, redundant resin would be collected by resin trap. At last when all the glass fiber was completely impregnated, the flow of resin would be stopped, and the mold was kept sealed under vacuum until the test specimen cures in room temperature.

2.1. Tests of stiffness and strength properties of laminate

Mechanical properties of the composite plates were determined experimentally at room temperatures. Test specimens were pre-

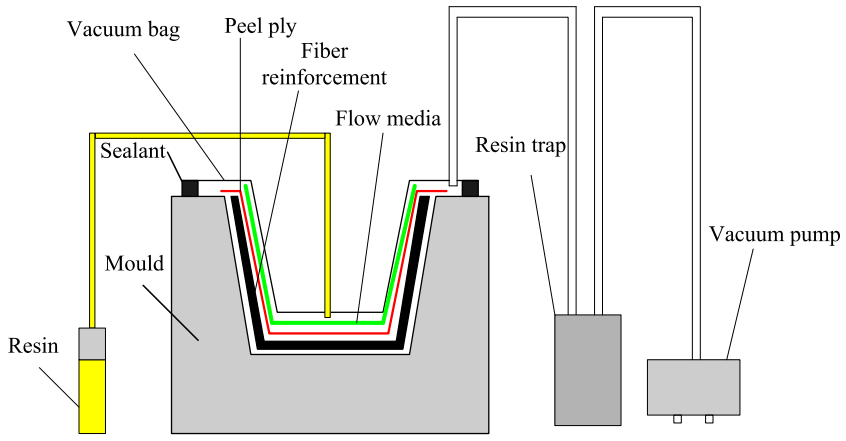

Fig. 2. Schematic diagram of VARI.

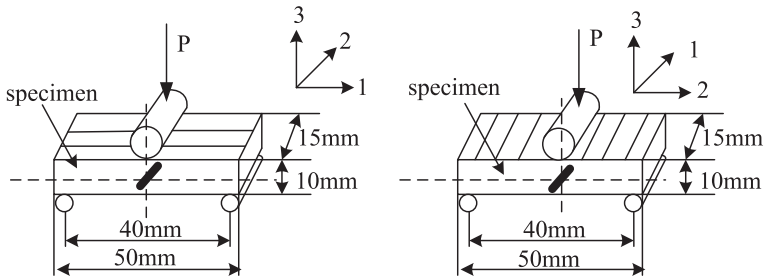

Fig. 3. Schematic views of three-point bending tests for G_{13} and G_{23}.

Table 1
Unidirectional stiffness properties for composite plate.

E_{11} (GPa)	E_{22} (GPa)	E_{33} (GPa)	G_{12} (GPa)	G_{13} (GPa)	G_{23} (GPa)	v_{12}	v_{13}	v_{23}
20	6.452	6.452	3.545	3.545	1.52	0.3	0.3	0.5

Table 2
Material strength data for composite plate.

X_T (MPa)	X_C (MPa)	Y_T (MPa)	Y_C (MPa)	S_{12} (MPa)	S_{13} (MPa)	S_{23} (MPa)
560	400	10.42	106	13.7	13.7	6

pared according to the ASTM standards. All the specimens were tested by Zwick/Roell mechanical testing machine.

Longitudinal Elastic modulus E_{11}, Poisson's ratio v_{12}, longitudinal tensile strengths X_T, transverse Elastic modulus E_{22} and transverse tensile strengths Y_T were measured by using longitudinal and transverse $[0^\circ]_8$ unidirectional composite specimens. The specimens were loaded up to the failure loads in the axial direction. Elastic modulus, E_{11} and E_{22} were calculated from the initial slope of the stress–strain curves. The tensile strengths of the unidirectional composite plates, X_T and Y_T, were determined by dividing the failure load to the cross-sectional area of the longitudinal and transverse specimens, respectively. The longitudinal and transverse compressive strengths, X_C and Y_C, are obtained by dividing the failure load to the cross-sectional area of the specimens.

To determine the out-plane shear modulus G_{13} and G_{23}, specimens with 15 mm width, 50 mm length and 10 mm thickness were manufactured by using the standard test method for short-beam strength as described in ASTM D2344/D2344M. The strain-gage was glued along the natural axis of longitudinal lateral surface of the specimen at angle of 45° with transverse direction as shown in Fig. 3 (in-plane 1–3 for G_{13}, in-plane 2–3 for G_{23}). Maximum shear stress in natural axis was calculated as given in Eq. (1). G_{13} and G_{23} can be calculated by using Eq. (3).

$$\tau_{13} = \frac{3P}{4A} \tag{1}$$

where A is the cross-sectional area and P is static force.

$$\gamma_{13} = 2\varepsilon \tag{2}$$

$$G_{13} = \frac{\tau_{13}}{\gamma_{13}} \tag{3}$$

The obtained results from the mechanical tests are given in Tables 1 and 2.

2.2. Failure tests of joints with different geometric parameters

Bolted-joint test configuration and geometry parameters under investigation in this study are shown in Fig. 4. The stacking sequence of laminate is $[0/0/+45/-45/0/90/0/+45/-45/0]_s$. 0° ply accounts for 50% of whole ply and 45° ply takes up 40%. Each ply thickness for this laminate is nominally 0.25 mm yielding a nominal laminate thickness of 5 mm. Composite laminate is made by VARI. Influence of geometric parameters on failure of joint is investigated. Geometric parameters are the distance from the free edge of plate to the diameter of bolt hole (E/D = 1, 2, 3, 4, and 5) ratio and the width of the specimen to the diameter of bolt holes (W/D = 2, 3, 4, and 5) ratios. Here the diameter of bolt-hole is 8 mm. Bolt torque is 6 N m.

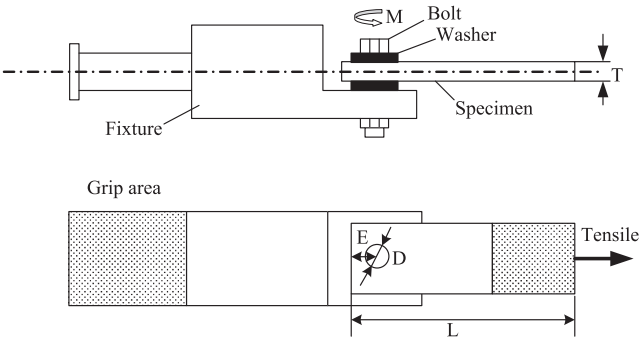

Fig. 4. Bolted-joint test configuration and geometry parameters.

As shown in Fig. 4, the test specimens are bolted with clamping apparatus, and clamping apparatus is clamped into a testing machine. In order to avoid stress concentration between test specimen and clamping apparatus, washers are placed between these two components. The load application was carried out on the end of specimen with a constant speed until joint collapse occurred. Force and displacement of the specimens are recorded. There are 5 groups of tests and a total of 20 specimens are tested. Failure load–displacement curves and failure modes of joints are shown in Fig. 5 and Table 3.

Experiments results in Fig. 5 show that with increase of geometric parameters, failure load increase obviously. But when W/D = 3 and E/D = 4, failure load reach the maximum value 16230 N, then

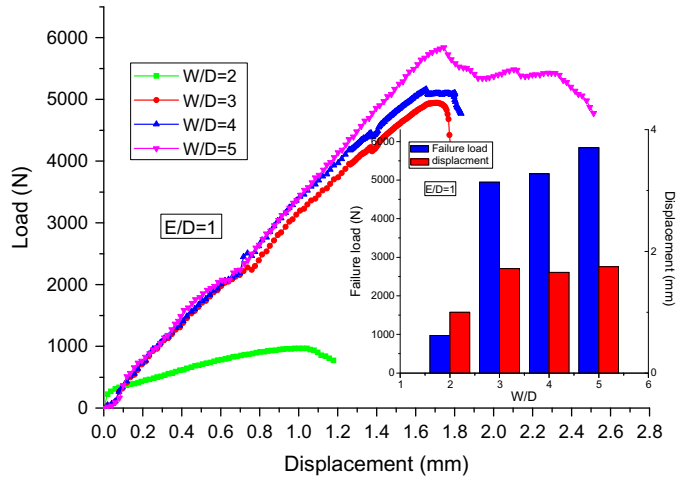

(a) E/D=1, W/D=2, 3, 4, 5

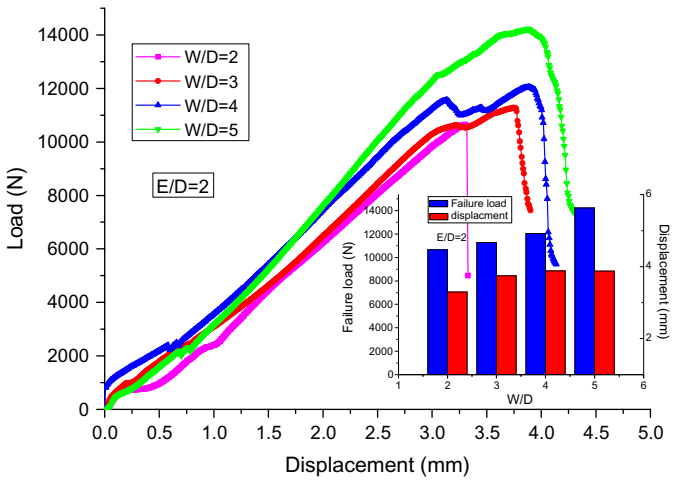

(b) E/D=2, W/D=2, 3, 4, 5

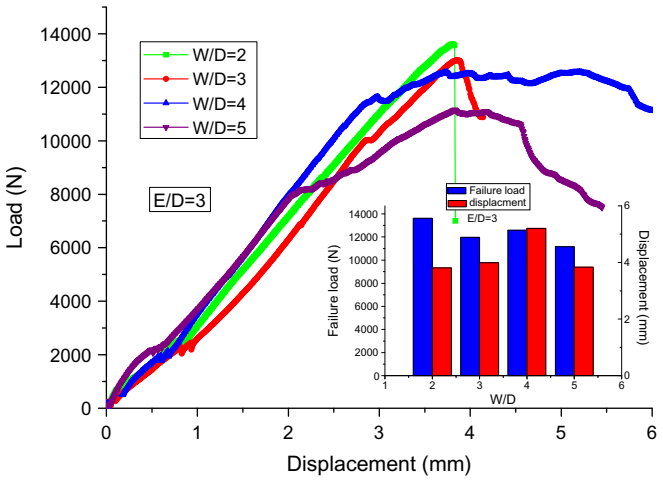

(c) E/D=3, W/D=2, 3, 4, 5

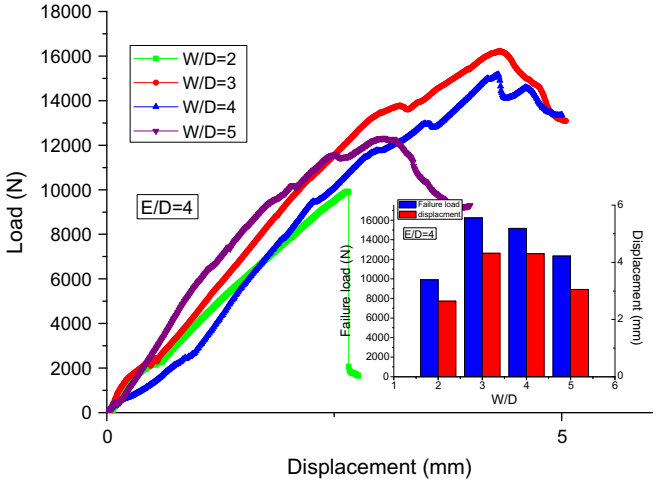

(d) E/D=4, W/D=2, 3, 4, 5

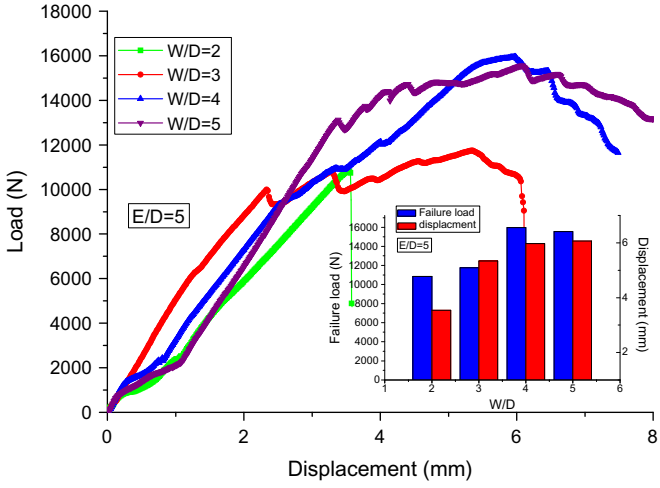

(e) E/D=5, W/D=2, 3, 4, 5

Fig. 5. Failure load–displacement curves and failure modes of joints with geometric parameters: W/D = 2, 3, 4, and 5 and E/D = 1, 2, 3, 4, and 5.

with increase of geometric parameters, failure load decrease gradually. When E/D = 1 and 2, nonlinear of displacement–load curves is not very obvious, but when E/D is greater than 2, nonlinear of displacement–load curve is quite serious. Fluctuations of curves indicate that failure modes of bolted composite joint become complicated, and bearing failure mode is the main factor of nonlinear. Compared with failure modes in Table 3, when geometric parameters ratios are small, the main failure modes are net-tension and cleavage. With the increase of geometric parameter ratio, mixed failure modes: net-tension, shear out and bearing are main failure

Table 3
Failure modes of joints.

	W/D			
E/D	2	3	4	5
1	C	S	S	S
2	N	B + S	B + S	B + S
3	N	B + S	B + S	B + S
4	N	B + S	B + S	B + S
5	N	N + S	B + S	B + S
Failure mode				

modes. Failure modes show an excellent agreement with nonlinear of displacement–load curves.

From bar chart of failure load and displacement in Fig. 5, it can be seen that in each group of geometric parameter test, $W/D = 4$ is a quite representative parameter. When $W/D = 4$, $E/D = 1$, 2, 3, and 4, failure loads are all second largest value, and $E/D = 5$, failure load reaches the maximum value. At the same time, displacement of joint failure is almost is the largest, which could avoid the sudden collapse of structure and is good for joint design.

3. Numerical study

Since the joint problem is contact finite element which is a three-dimensional problem, and traditional composite laminate is treat as shell which cannot solve the contact problem well. In this work, two finite element models are developed in ABAQUS/Standard and Explicit to simulate failure of joints. 3D Hashin criteria is used in two different progress failure models which use three-dimensional finite element method and solve contact finite problem well. Here, geometric parameters: $E/D = 2$, $W/D = 2$, 3, 4, and 5 are chosen as simulation targets. Experimental results and simulation results are compared with each other and joint progressive failure progress is explained in detail.

3.1. Model developed in ABAQUS/Standard

ABAQUS is good at structure nonlinear analysis, ABAQUS/Standard is often used to solve static or quasi-static finite element problem. Tensile of joint could be treated as static problem, so the first progressive failure model is developed in ABAQUS/Standard. The joint model is simplified as one bolt and laminate.

Since the diameter of bolt D is 8 mm, $W/D = 2$, 3, 4, and 5 and $E/D = 2$, so W and E can be calculated by geometric parameters ratio. The stacking sequence of laminate is $[0/0/+45/-45/0/90/0/+45/-45/0]_s$. Each ply thickness for this laminate is nominally 0.25 mm yielding a nominal laminate thickness of $T = 5$ mm. According to above geometric parameters, model can be built. Then each ply material properties are applied in model according to data in Table 1. Since the joint is contact problem and bolt torque need to be applied in bolt, so load step should be applied in model step by step. As shown in Fig. 6, (1) laminate is fixed, contact property and bolt torque is applied in model, respectively, friction coefficient is 0.2 and bolt torque is 6 N m. (2) Keep bolt length and laminate fixed. (3) Keep bolt fixed and set laminate free. (4) Prescribed displacement in the x-direction is applied to the end of laminate. After model is completed, the model is meshed by C3D8R: an 8-node linear brick, reduced integration element. At last user subroutine USDFLD is called to solve the ABAQUS/Standard progressive model.

Progressive model using USDFLD which is used to determine the failure loads and the failure modes, must has a failure criteria. The 3D Hashin failure criteria is used. The failure criterion for each mode is as follows.

Tensile matrix failure, $\sigma_{22} + \sigma_{33} > 0$.

$$\frac{1}{Y_T^2}(\sigma_{22}+\sigma_{33})^2 + \frac{1}{S_{23}^2}(\sigma_{23}^2 - \sigma_{22}\sigma_{33}) + \frac{1}{S_{12}^2}(\sigma_{12}^2+\sigma_{13}^2) = 1 \tag{4}$$

Compressive matrix failure, $\sigma_{22} + \sigma_{33} < 0$.

$$\frac{1}{Y_C}\left[\left(\frac{Y_C}{2S_{23}}\right)^2 - 1\right](\sigma_{22}+\sigma_{33}) + \frac{1}{4S_{23}^2}(\sigma_{22}+\sigma_{33})^2 + \frac{1}{S_{23}^2}(\sigma_{23}^2 - \sigma_{22}\sigma_{33}) + \frac{1}{S_{12}^2}(\sigma_{12}^2+\sigma_{13}^2) = 1 \tag{5}$$

Tensile fiber failure, $\sigma_{11} > 0$.

$$\left(\frac{\sigma_{11}}{X_T}\right)^2 + \frac{1}{S_{12}^2}(\sigma_{12}^2+\sigma_{13}^2) = 1 \tag{6}$$

Compressive fiber failure, $\sigma_{11} < 0$.

$$\left(\frac{\sigma_{11}}{X_C}\right)^2 = 1 \tag{7}$$

The above failure criterion used in subroutine USDFLD allows material properties to be a direct function of predefined field variables. Flowchart of the progressive damage model is shown in

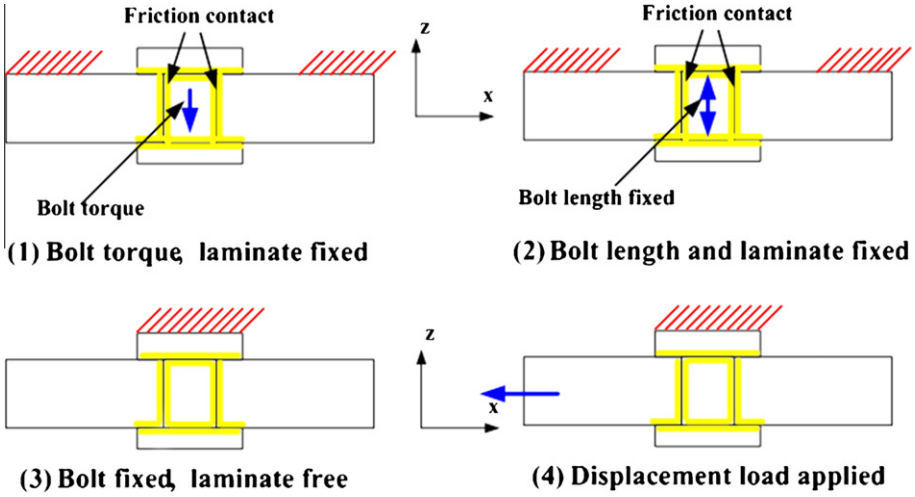

Fig. 6. Load steps for finite element model.

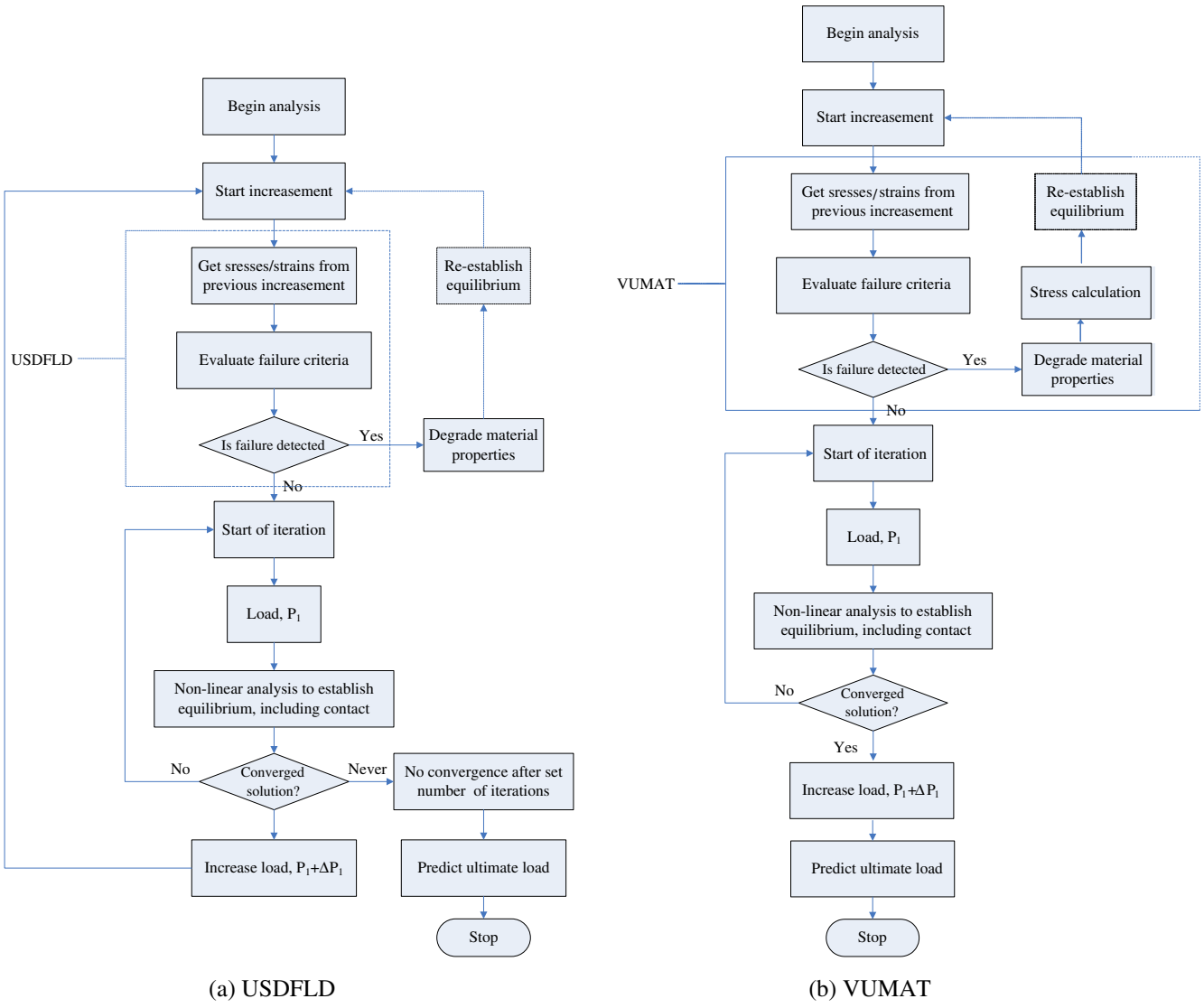

Fig. 7. Flowcharts of progressive damage models.

Table 4
Stiffness degradation rule in USDFLD.

	E_{11} (%)	E_{22} (%)	E_{33} (%)	G_{12} (%)	G_{13} (%)	G_{23} (%)	v_{12} (%)	v_{13} (%)	v_{23} (%)
Tensile matrix mode		10	10			10			10
Compressive matrix mode		10	10			10			10
Tensile fiber mode	10			10	10		10	10	
Compressive fiber mode	10			10	10		10	10	
More than one failure mode	10	10	10	10	10	10	10	10	10

Table 5
Stiffness degradation rule in VUMAT.

	E_{11} (%)	E_{22} (%)	E_{33} (%)	G_{12} (%)	G_{13} (%)	G_{23} (%)	v_{12}	v_{13}	v_{23}
Tensile matrix mode		1	1	1		1	0		0
Compressive matrix mode		1	1	1		1	0		0
Tensile fiber mode	1			1	1		0	0	
Compressive fiber mode	1			1	1		0	0	

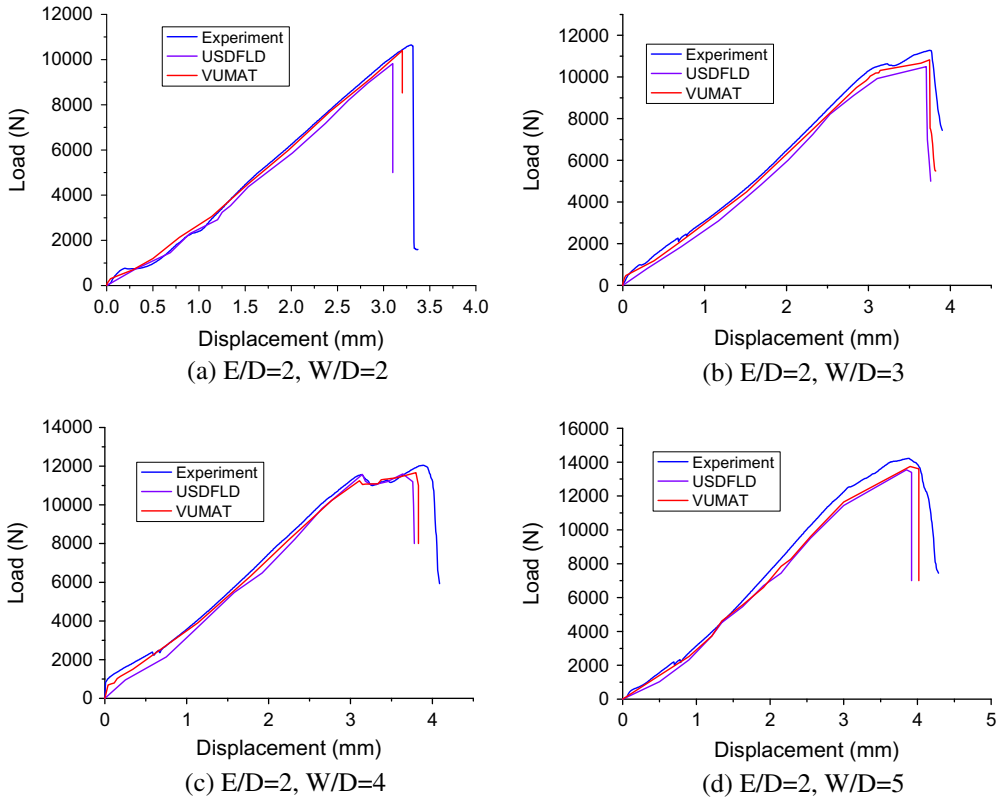

Fig. 8. Comparison of simulation results and experiments with $W/D = 2$, 3, 4, and 5 and $E/D = 2$.

Fig. 7a. Stresses from the previous increment are called into the subroutine at the beginning of the current increment and used to evaluate Hashin failure criteria (Eqs. (4)–(7)). Once the failure criteria are satisfied, the field variables are updated and used to reduce the material properties to 10% of their original stiffness according to the scheme shown in Table 4.

3.2. Model developed in ABAQUS/Explicit

During tensile test of composite joint, displacement is applied to joint with constant speed, and this process could be treat as a dynamic finite element problem, so progressive failure model developed in ABAQUS/Explicit also could be used to simulate failure of joint. User subroutine VUMAT is implemented in this model.

In Explicit progressive failure model, material properties are shown in Table 1 and boundary condition are same as the Standard model. Difference between these two models is that ABAQUS/Explicit is used in finite element analysis of Explicit model, so the step module should change with model. The load steps applied for model are shown in Fig. 6.

User subroutine USDFLD allows material properties to be a direct function of predefined field variables, however, user subroutine VUMAT is used to define the mechanical constitutive behavior of a material. As shown in Flowchart Fig. 7b, when analysis iteration starts, subroutine VUMAT is called into model to evaluate Hashin failure criteria (Eqs. (4)–(7)). Once the failure criteria are satisfied, the state variables are updated and material stiffness is reduced according to the scheme shown in Table 5. Different with USDFLD, mechanical constitutive behavior of a material will be defined in VUMAT. Damage stiffness matrix will be calculated and new element stress will be calculated by damage stiffness. This process does not need to be calculated in ABAQUS, so calculation time will be obviously reduced and the convergence speed will be improved greatly.

3.3. Finite element simulation results and analysis

As shown in Fig. 8, $W/D = 2$, 3, 4, and 5 and $E/D = 2$, experiments results and two finite element simulation results are compared with each other. As can be seen, remarkably close agreement is obtained between simulation and experiment. Compare with experiment results, error of failure load of model developed in ABAQUS/Standard is about from 4% to 7.6%, and error of failure load of model developed in ABAQUS/Explicit is 2–4%. Discrepancies between numerical and experimental results in Fig. 8 are made by the reasons as follow: (1) Since the single-lap joint is simplified as one bolt and laminate, washer and bolt are treat as one component. In fact, washer could increase contact area and friction, and reduce stress concentration. (2) Meanwhile, since the stiffness degradation occurs at failure moment, residual stiffness still could carry load. Considering above reason, discrepancies between numerical and experimental results are reasonable.

In Fig. 8, compared with two element finite simulation results, it can be seen that Explicit model has higher accuracy than Standard model. Progressive failure of joint is shown in Fig. 9. Here $W/D = 4$ and $E/D = 2$, field variable and state variable are used to represent damage of joint in Standard and Explicit model, respectively. Compared with experimental result, failure mode of joint is mixed failure mode: shear out and bearing. Shear out is observed by fiber failure, and bearing can be represented by matrix failure. Simulation results show an excellent agreement with experimental results. Although failure of joints could be simulated by two kinds of finite element model well, model developed in ABAQUS/Explicit can save more calculation time, and improve convergence speed and accuracy.

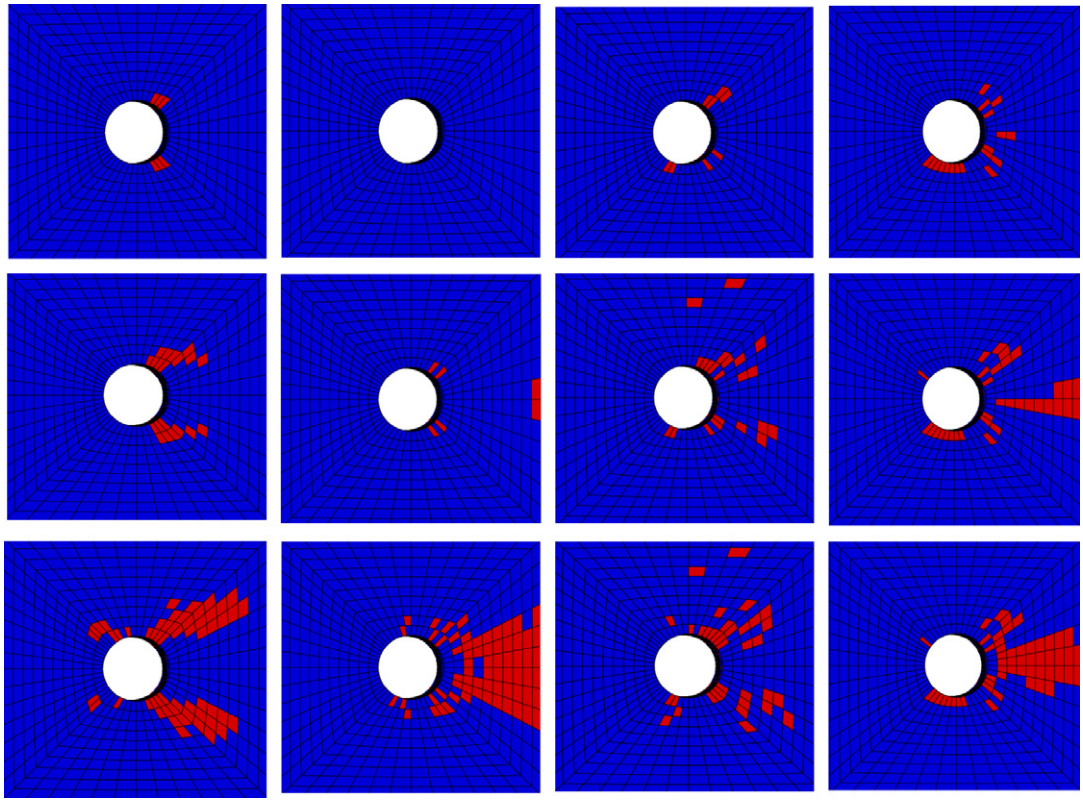

Fig. 9. Progressive failure of two different models with $W/D = 4$ and $E/D = 2$.

4. Conclusions

In this study, influence of geometric parameters on failure response of bolted single-lap composite joints is investigated by experiments and finite element methods. Since VARI process cures in room temperature and enable the manufacture of large structures with high mechanical properties under vacuum. So VARI is chosen as the molding process of specimens in experiments. To predict failure of joint, two kinds of progressive failure models are developed in ABAQUS, using subroutines USDFLD and VUMAT, respectively. Simulation results show an excellent agreement with experimental results.

From the experimental results and finite element analysis, it can be concluded that:

- The bolted joints made by VARI process have enough strength, and maximum failure load is 16230 N, when $W/D = 3$ and $E/D = 4$. Considering failure displacement and failure load, $W/D = 4$ is a better choice for bolted composite joint design.
- When E/D increases from 4 to 5, the failure load does not increase obviously, which indicates that during design of bolted composite joint, geometric parameters should be chosen properly. Large geometric parameter does not mean high strength.
- In the experiments, $E/D = 4$ or 5, the main failure modes is mixed failure mode which is shear out and bearing. Mixed mode reduces the sudden of failure occurrence, and it is convenient for repair and maintenance of structure.
- Two kinds of progressive failure models predict the failure of joint well. Finite element analysis results show an excellent agreement with experimental results. Model developed in ABAQUS/Explicit is found to be robust, accurate and highly efficient.

Acknowledgements

This work has been funded by Fundamental Research Funds for the Central University (No. HEUCFZ1003), General Program of National Natural Science Foundation of China (No. 11272096) and Research Fund for the Doctoral Program of Higher Education of China (No. 20112304110015).

References

[1] Picard A, Massicotte B, Boucher E. Strengthening of reinforced concrete beam with composite materials: theoretical study. Compos Struct 1995;33:63–75.
[2] Growth-GRD1-10216. Bolted joints in composite aircraft structures (BOJCAS). Brussels; 1999.

[3] Dano Marie-Laure, Kamal Elhassania, Gendro Guy. Analysis of bolted joints in composite laminates: strains and bearing stiffness predictions. Compos Struct 2007;79:562–70.
[4] Wang Zhenqing, Zhou Song, Zhang Jifeng, Wu Xiaodi, Zhou Limin. Progressive failure analysis of bolted single-lap composite joint based on extended finite element method. Mater Des 2012;37:582–8.
[5] McCarthy MA, McCarthy CT, Lawlor VP, Stanley WF. Three-dimensional finite element analysis of single-bolt, single-lap composite bolted joints: Part I—Model development and validation. Compos Struct 2005;71:140–58.
[6] McCarthy MA, McCarthy CT, Lawlor VP, Stanley WF. Three-dimensional finite element analysis of single-bolt, single-lap composite bolted joints: II––Effects of bolt-hole clearance. Compos Struct 2005;71:159–75.
[7] Gray PJ, McCarthy CT. A global bolted joint model for finite element analysis of load distributions in multi-bolt composite joints. Compos Part B. 2010;41:317–25.
[8] McCarthy CT, Gray PJ. An analytical model for the prediction of load distribution in highly torqued multi-bolt composite joints. Compos Struct 2011;93:287–98.
[9] Sen Faruk, Pakdil Murat, Sayman Onur, Benli Semih. Experimental failure analysis of mechanically fastened joints with clearance in composite laminates under preload. Mater Des 2008;29:1159–69.
[10] Kapti Servet, Sayman Onur, Ozen Mustafa, Benli Semih. Experimental and numerical failure analysis of carbon/epoxy laminated composite joints under different condition. Mater Des 2010;31:4933–42.
[11] Olmedo Álvaro, Santiuste Carlos. On the prediction of bolted single-lap composite joints. Compos Struct 2012;94:2110–7.
[12] Li Hongshuang, Lu Zhenzhou, Zhang Yi. Probabilistic strength analysis of bolted joints in laminated composites using point estimate method. Compos Struct 2009;88:202–21.
[13] Dano Marie-Laure, Kamal Elhassania, Gendron Guy. Analysis of bolted joints in composite laminates: strains and bearing stiffness predictions. Compos Struct 2007;79:562–70.
[14] Dano Marie-Laure, Gendron Guy, Picard Andre. Stress and failure analysis of mechanically fastened joints in composite laminates. Compos Struct 2000;50:287–96.
[15] Hühne C, Zerbst A-K, Kuhlmann G, Steenbock C, Rolfes R. Progressive damage analysis of composite bolted joints with liquid shim layers using constant and continuous degradation models. Compos Struct 2010;92:189–200.
[16] Francesco Ascione, Feo Luciano, Maceri Franco. An experimental investigation on the bearing failure load of glass fibre/epoxy laminates. Compos Part B 2009;40:197–205.
[17] Ascione Francesco, Feo Luciano, Maceri Franco. On the pin-bearing failure load of GFRP bolted laminates: an experimental analysis on the influence of bolt diameter. Compos Part B 2010;41:482–90.
[18] Feo Luciano, Marra Gianfranco, Mosallam Ayman S. Stress analysis of multi-bolted joints for FRP pultruded composite structures. Compos Struct 2012;94:3769–80.
[19] Brouwer WD, van Herpt ECFC, Labordus M. Vacuum injection moulding for large structural applications. Compos Part A 2003;34:551–8.
[20] Himmel N, Bach C. Cyclic fatigue behavior of carbon fiber reinforced vinylester resin composites manufactured by RTM and VARI. Int J Fatigue 2006;28:1263–9.